Fork sensing and strand switching control antagonistic activities of RecQ helicases

Daniel Klaue, Daniela Kobbe, Felix Kemmerich, Alicja Kozikowska, Holger Puchta, Ralf Seidel

Supplementary Information

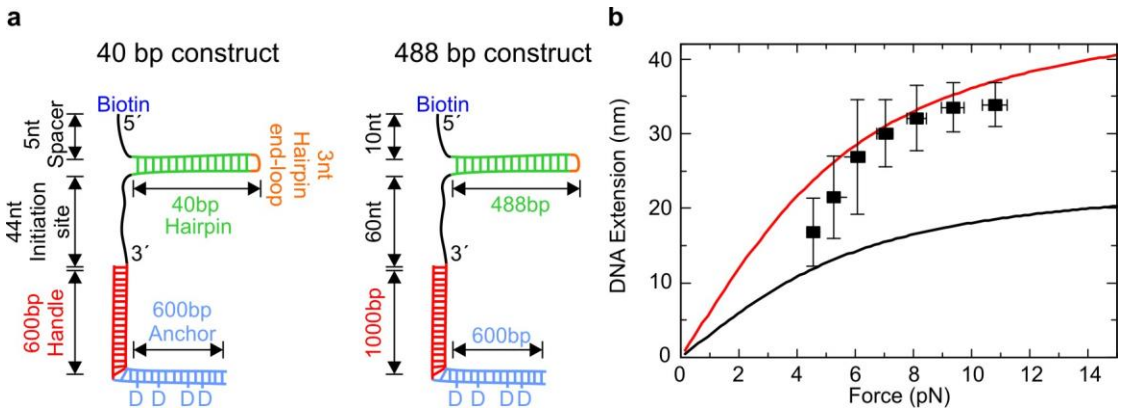

Supplementary Figure S1 | DNA hairpin constructs used for the experiments. (**a**) Schematic drawing of the used hairpin construct. On the 5´ end of the hairpin the construct is attached to a streptavidin coated magnetic bead (not in the sketch) through a biotin modification. The hairpin (green) contains 40, 90 or 488 base pairs (depending on the experiment). At the 3´ end of the hairpin a ssDNA overhang (e.g. 44 nt in the 40 bp construct, polydT, black) provides the entry site for the helicase. A dsDNA handle (~600 bp in the 40 bp construct, red) keeps the distance to the flow cell surface. The whole construct is immobilized to the anti-digoxigenin coated surface of the fluidic cell through an anchor (blue) containing several digoxigenin modified bases. (**b**) Average maximum DNA extension change as function of force during unwinding of the 40 bp long hairpin by AtRECQ2 (black squares). Solid lines show theoretical predictions for the DNA extension change according to the extensible freely jointed chain model[51] for 83 (red) and 43 nts (black) contour length. For both predictions a segment length of 1.5 nm and an elastic modulus of 530 pN[10] was taken. Below 10 pN secondary structure formation of the ssDNA shortens the average measured length[52]. The data suggests that AtRECQ2 unwinds the full 40 bp hairpin, without ssDNA loop formation (see main text). The measured extension data allows for the conversion of nanometers to base pairs at the particular forces. Error bars represent S.E.M. (*n* = 19, 19, 25, 156, 167, 166, 35 for increasing forces).

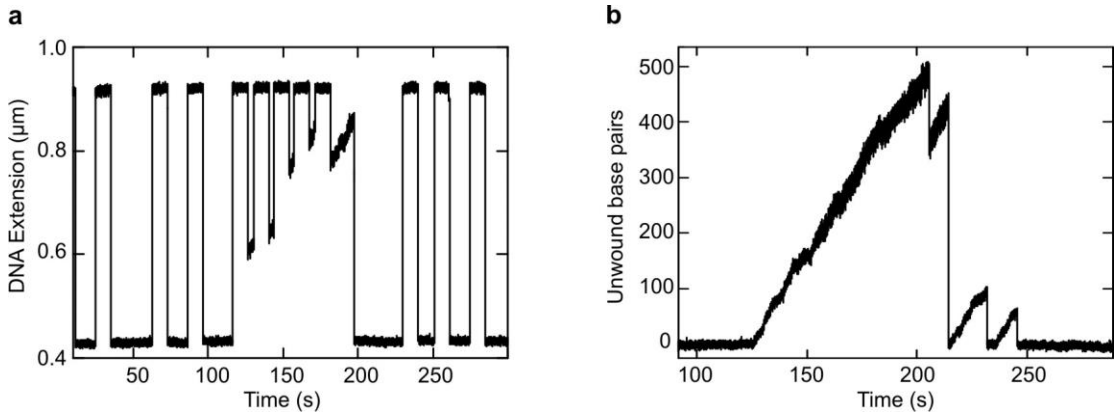

Supplementary Figure S2 | Single molecule conditions during unzipping and unwinding experiments. (**a**) Mechanical unzipping-rezipping cycles of a 488 bp hairpin between 7 and 20 pN in presence of AtRECQ2. Multiple successive cycles with no detectable enzyme on DNA interchanged with successive cycles of continuously bound enzyme providing additional evidence for the activity of a single enzyme-complex on DNA during these experiments. This is similar to the bursts of repetitive unwinding in Fig.1C (main text). Experimental conditions are as given in Methods. (**b**) AtRECQ2 is able to unwind several hundreds of base pairs. A force of 11 pN was applied in the experiment.

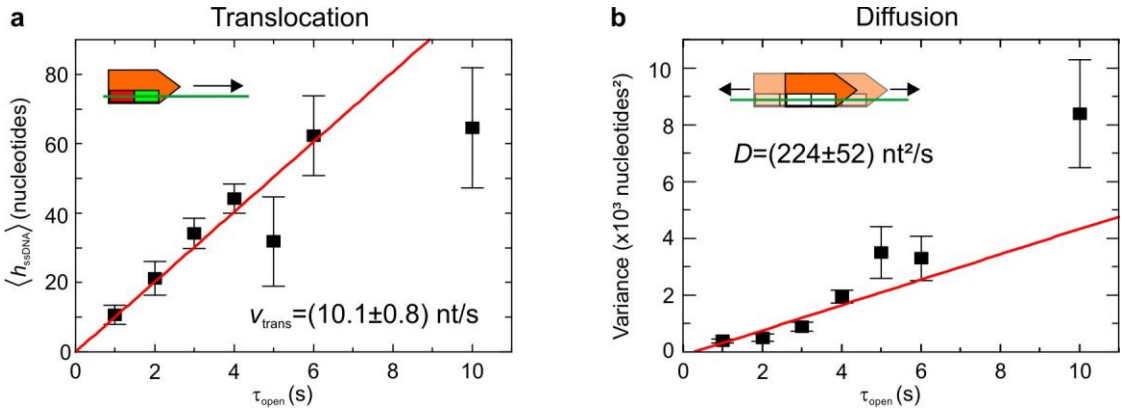

Supplementary Figure S3 | Mean and variance calculated for the distances AtRECQ2 moved on ssDNA. (**a**) Mean distance the enzyme moved on ssDNA for varying τ_{open} (filled squares). Error bars indicate the standard error of the mean. The red line is a linear fit to the data weighted with the errors. It reveals an average velocity for the forward movement of 10 nt/s. This value is lower than the true ssDNA translocation velocity since the enzyme most likely alternates between ssDNA translocation and diffusion (see main text) and thus spends only a fraction of τ_{open} for translocation. (**b**) Variance of the distance the enzyme on ssDNA for varying τ_{open} (filled squares). Error bars indicate standard error of the mean. The red line is a linear fit to the data weighted with the errors from which a lower bound for the diffusion coefficient of 225 nt²/s is estimated since the enzyme spends only a fraction of τ_{open} for diffusion. Values were calculated from the data in Figure 2B (main text). Error bars represent S.E.M. (n = 70, 30, 66, 151, 30, 35, 39 for increasing τ_{open} in both graphs).

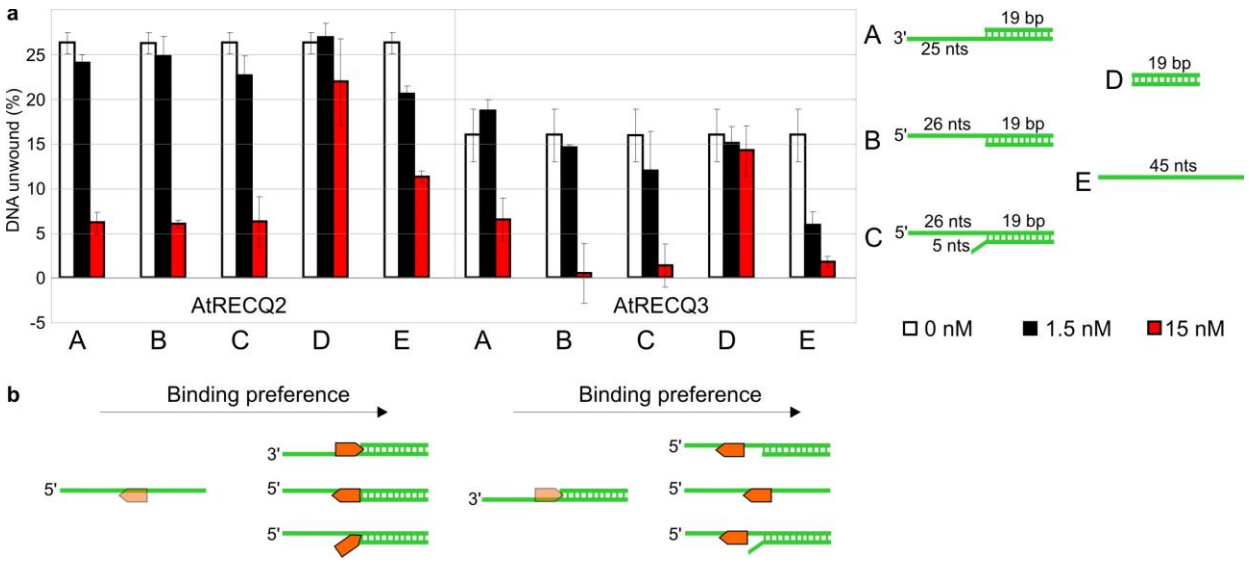

Supplementary Figure S4 | AtRECQ2 and AtRECQ3 preferentially bind to different structures. (**a**) The unwinding efficiency of 7 nM enzyme (AtRECQ2 left side, AtRECQ3 right side) with the radioactive labeled 25 nt 3' overhang substrate was determined as described for Fig. 3d during 1 min incubation in the presence of increasing concentrations of different unlabeled DNA structures as competitors as depicted (A to E). The reaction was started by mixing the enzyme with the other pre-mixed reaction components. As expected, the blunt end dsDNA competitor (D) shows the least influence on the unwinding reactions, indicative for non or non stable binding of the enzymes to dsDNA. In contrast the unwinding reaction of AtRECQ2 is partially reduced by high concentrations of single stranded DNA (E). The inhibition is even more pronounced in the presence of either 3' overhang (A), 5' overhang (B) or the splayed arm structure (C). This leads to the conclusion that AtRECQ2 preferentially binds to the junction point as sketched in **b**. This is in line with the model of junction sensing and AtRECQ2 preferentially orienting itself towards junction unwinding. Similar experiments also demonstrated a higher specificity for ss/dsDNA junctions than ssDNA and dsDNA for UvrD[18].
In contrast, unwinding of the 3' overhang by AtRECQ3 is most inhibited by the 5' overhang (B), single stranded DNA (E) or the flap structure (C) in the reaction, while the inhibition is less pronounced with the 3' overhang (A) substrate. This supports the model that AtRECQ3 is rather a rewinder than unwinder und preferentially translocates on ssDNA away from the junction. (**b**) Schematic overview of the binding preferences of AtRECQ2 (left) and AtRECQ3 (right). Faint and bright color of the helicase symbol (orange) represent weak and strong binding preference, respectively.

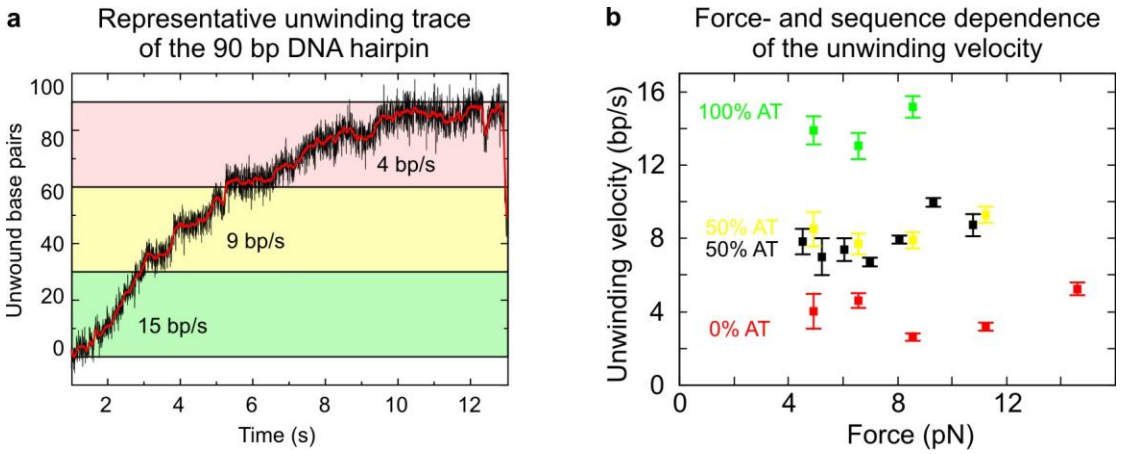

Supplementary Figure S5 | Force- and sequence dependence of AtRECQ2 unwinding velocity. (**a**) Representative trace of AtRECQ2 unwinding a DNA hairpin construct with three regions of different AT content (100% AT (green), 50% AT (yellow), 0% AT (red)). Unwinding events show decreasing unwinding velocities from high to low AT content. To determine the sequence-dependent unwinding velocity, only those unwinding events were chosen for which the DNA hairpin was completely unwound. The unwinding event was divided into three 30 bp long stretches and the velocity for each stretch was determined independently. (**b**) Unwinding velocity as function of the applied force for the regions with different AT content (as indicated). The black data points are obtained from measurements using the 40 bp long DNA hairpin (e.g. as used in Fig. 1), which also contains 50% AT base pairs. Error bars indicate the standard error of the mean. While a region composed only of AT bps is unwound with approximately 15 bp/s, a pure GC region slows the helicase down to 4 bp/s. This is characteristic for so called passive helicases that use mainly the breathing of the bp at the junction for the forward stepping [21,53]. For such helicases, the unwinding velocity exhibits additionally a strong force dependence, since the external tension supports the opening of the bp[10,11,32]. In contrast to this, AtRECQ2 is only weakly force dependent for all investigated sequences. A simple explanation for this apparent contradiction is provided by the clamping of the unwinding fork by the enzyme itself. This should shield the unwinding fork from the influence of the external force, making the bp opening and thus the unwinding velocity of the helicase only dependent on the DNA sequence. Error bars represent S.E.M. ($17 < n < 167$).

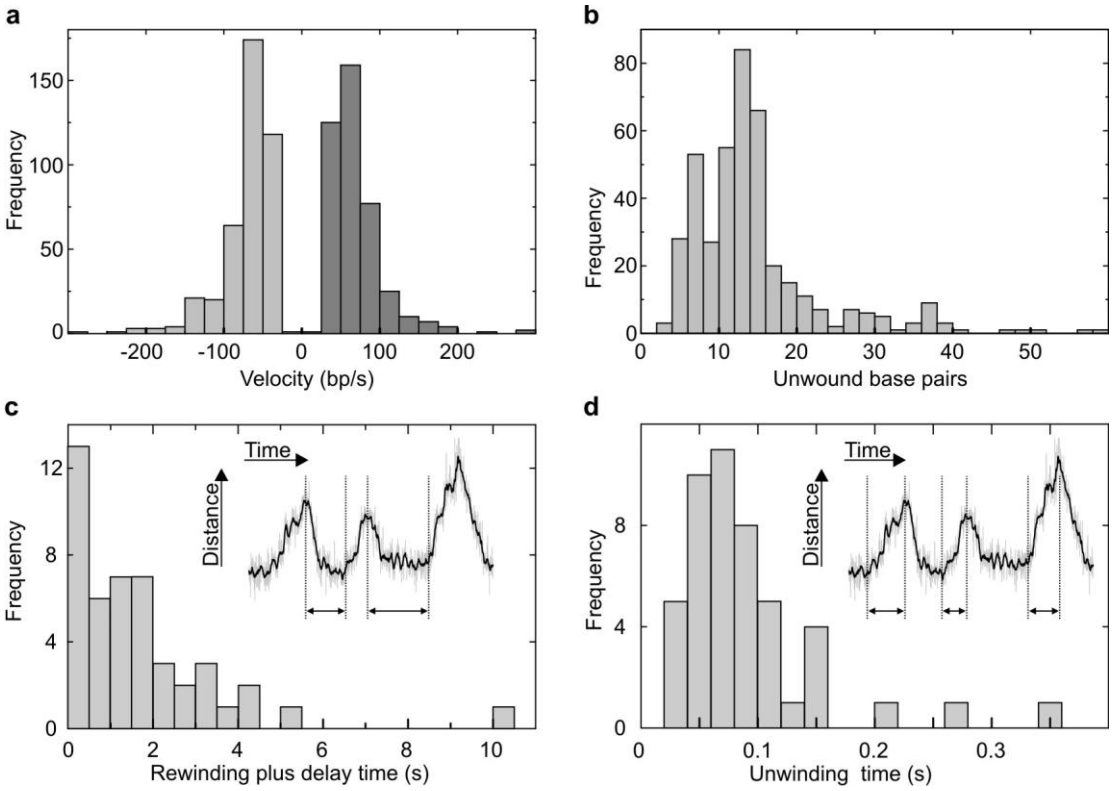

Supplementary Figure S6 | Analysis of the un- and rewinding events of AtRECQ3. (**a**) Histogram of the unwinding- (dark gray bars) and rewinding (light gray bars) velocities of AtRECQ3 on the 488 bp hairpin at 11.9 pN as determined from linear fits to single un-/rewinding events. A mean unwinding velocity of 70±2 bp/s and a mean rewinding velocity of 69±2 bp/s are obtained. (**b**) Histogram of the number of unwound base pairs per single event of AtRECQ3 on the 488 bp hairpin at 11.9 pN. The values are broadly distributed with a mean of 14.6±0.4 bp. (**c**) Histogram of the time period between the start of rewinding and initiation of a new unwinding event (rewinding time plus delay time) between two successive events (see sketch). This reflects the time the enzyme requires to switch from rewinding to unwinding providing a mean of 1.8±0.3 s. (**d**) Histogram of the time the enzyme spends on unwinding (see sketch). This reflects the time the enzyme requires to switch from unwinding to rewinding providing a mean of only 0.09±0.01 s.

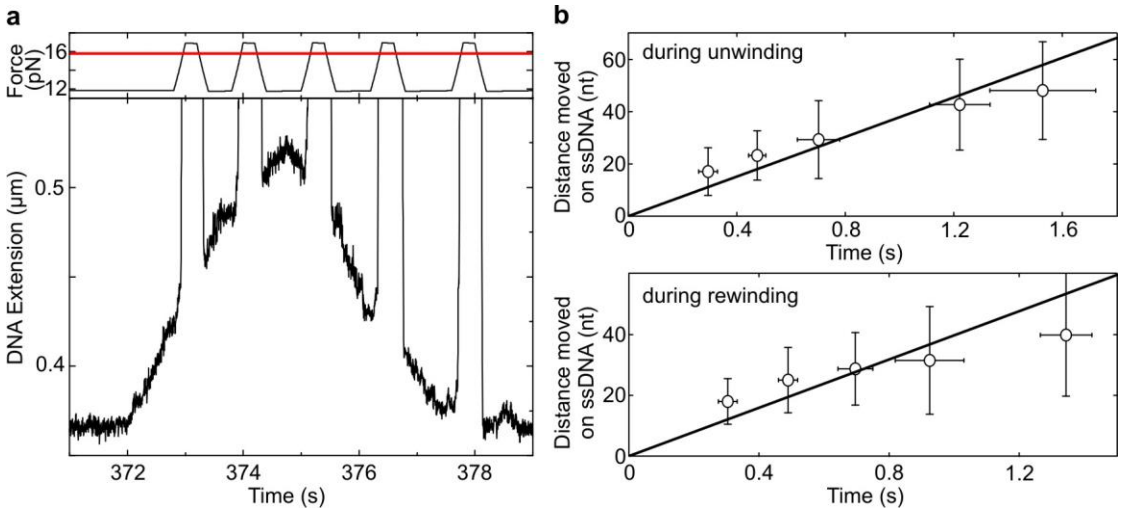

Supplementary Figure S7 | AtRECQ3 translocates along ssDNA. (**a**) A 488 bp long DNA hairpin (*F*unzip=15.8 pN, upper graph red solid line) is mechanically un- and rezipped by switching the force between *F*=11.8 pN (hairpin closed) and *F*=16.9 pN (hairpin open), as explained in the main text (see also Figure 2A). During the unzipping periods AtRECQ3 continues to translocate on the ssDNA in the same direction as during unwinding. Thus it shows unidirectional behavior. (**b**) Mean moved distance of AtRECQ3 on ssDNA during unwinding (upper) and rewinding (lower) as function of time. Linear fits to the data provide mean ssDNA translocation velocities for unzipping during unwinding of 38±4 nt/s and rewinding of 40±5 nt/s, which are the same within error. Interestingly, the ssDNA translocation velocity is slower than the unwinding velocity. Error bars represent S.D. (*n* = 70, 161, 76, 67, 31 for unwinding and *n* = 102, 169, 84, 32, 17 for rewinding).

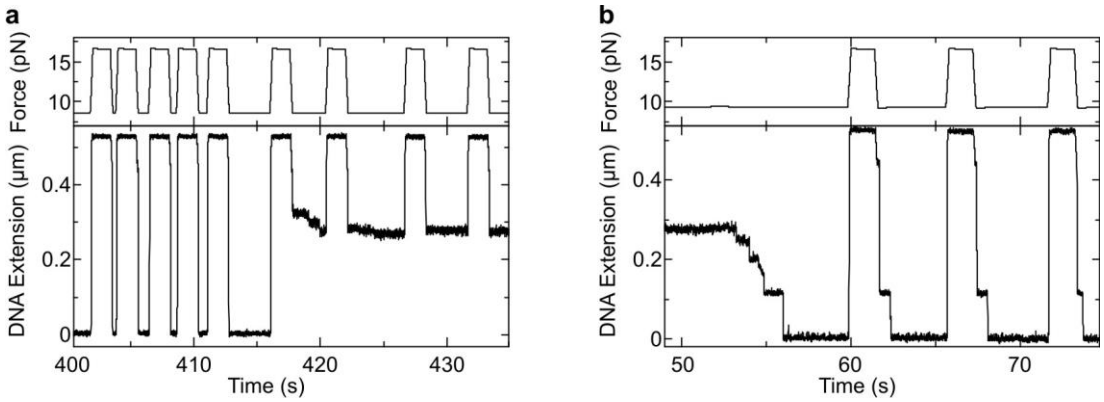

Supplementary Figure S8 | Processive DNA rewinding by AtRECQ3 requires ATP hydrolysis. (**a**) Unzipping and rezipping of the 488 bp hairpin in presence of AtRECQ3, but absence of ATP. The enzyme is able to bind to the ssDNA when the hairpin is open and prevents full rezipping of the hairpin. Instead of rewinding, the enzyme stays at a fixed position. (**b**) The stepwise rezipping of the hairpin could arise from either dissociation of the AtRecQ3 followed by stopping due to the next bound enzyme or an occasional release of the enzyme during which it gets pushed along the ssDNA until it attaches again.

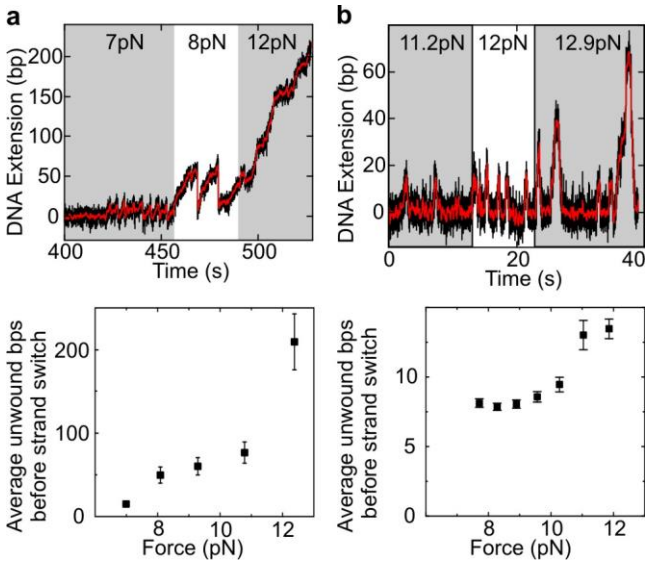

Supplementary Figure S9 | The unwinding lengths of AtRECQ2 and AtRECQ3 are controlled by force. (**a**) (upper) DNA unwinding of the 488 bp hairpin by AtRECQ2 at different forces as indicated in the figure. The DNA length was recorded at 300 Hz (black line). The red line shows the data filtered with a 10 Hz moving average. (lower) Mean unwinding length as function of force for AtRECQ2. Error bars indicate the standard error of the mean. (**b**) Force dependence of the unwinding length on the 488 bp hairpin of AtRECQ3. Plots and labels are as in **a,** i.e. (upper) Unwinding time trajectoiry at different forces and (lower) Mean unwinding length. The mean unwound base pairs before strand switching reach a plateau at low forces, while their distributions (see e.g. Supplementary Fig. S7b) remain broad. This is different to HsBLM that exhibited a rather defined unwinding distance suggesting that it can measure the distance before strand switching[16].

Both enzymes unwind significantly more bp with higher applied forces (Fig. 6). AtRECQ2 is even capable of completely unwinding the full 488 bp long hairpin (Supplementary Fig. S2b). This is in strong contrast to bulk strand displacement experiments, were only a few 10s of bp are separated[7], which was interpreted as limited processivity. Considering our results and our model for DNA unwinding by the studied helicases, we suggest that high forces do not prolong the DNA unwinding directly, but rather suppress strand switching from unwinding to rewinding or abrupt resetting. Intuitively this is sensible, since the force is physically keeping the two hairpin ends away from each other, which may inhibit this transition.

Supplementary references

51. Smith, S.B., Finzi, L. & Bustamante, C. Direct mechanical measurements of the elasticity of single DNA molecules by using magnetic beads. *Science* **258**, 1122–1126 (1992).

52. Dessinges, M.N. *et al*. Stretching single stranded DNA, a model polyelectrolyte. *Phys Rev Lett* **89**, 248102 (2002).

53. Betterton, M.D. & Julicher, F. Opening of nucleic-acid double strands by helicases: Active versus passive opening. *Physical Review E* **72**, 11904 (2005).